Available online at www.sciencedirect.com
ScienceDirect
Trans. Nonferrous Met. Soc. China 28(2018) 1287−1297
Transactions of Nonferrous Metals Society of China
www.tnmsc.cn

Effect of post-weld heat treatment on joint properties of dissimilar friction stir welded 2024-T4 and 7075-T6 aluminum alloys

B. SAFARBALI, M. SHAMANIAN, A. ESLAMI

Department of Materials Engineering, Isfahan University of Technology, Isfahan 84156-83111, Iran

Received 20 April 2017; accepted 11 August 2017

Abstract: The effect of post-weld heat treatment on dissimilar friction stir welded AA7075 and AA2024 joints was studied. After welding in constant parameters, solution heat treatment and various aging treatments were given to the welded joints. Microstructural and phase characterizations were done using optical microscope, SEM, FE-SEM, XRD and EDS techniques. Finally, mechanical properties of post-weld heat treated joints were evaluated and compared with as-welded joints. Results show that both 2024-T6 and 7075-T6 post-weld heat treatment procedures considerably improve the mechanical strength of the welded joint, with higher strength obtained for the 7075-T6 procedure, in comparison with the as-welded joint. This is explained by the formation of fine precipitates during the aging process, despite the abnormal grain growth. Fracture occurs at the interface between thermo- mechanical affected zone (TMAZ) and heat affected zone (HAZ) on the retreating side (AA7075) of as-welded joint, while by applying post-weld heat treatment fracture location shifts towards the stir zone (SZ) of the welded joint. Also, for post-weld heat treated samples, fracture surface is predominantly inter-granular, while in as-weld joint, fracture surface is mostly trans-granular. This is explained by dissolution and coarsening of precipitates within grains in post-weld heat treated joints.

Key words: friction stir welding; dissimilar welds; post-weld heat treatment; microstructure; mechanical properties

1 Introduction

AA2024 and AA7075 alloys are the two main aluminum alloys, which are widely used in the aerospace industry due to high strength, low density, high fracture toughness and good thermal stability microstructures [1]. The need for joining dissimilar materials is growing in various industries because of the requirement of components to withstand complex loading conditions [2]. In common fusion welding techniques, the alloys show defects such as porosity, hot crack, reduction in strength and flexibility in welded area [1]. Friction stir welding (FSW) is a solid state metal joining technique that was developed by The Weld Institute of Cambridge, UK [3]. In this method, the generated temperature from rotation of the tool does not exceed the melting point of the work piece and mentioned problems in fusion welding are not significant. FSW method is particularly suitable for joining of aluminum alloys with poor weld-ability, such as 2xxx and 7xxx series [4].

Microstructure of aluminum alloys in FSW normally involves nugget zone (NZ), thermo-mechanical affected zone (TMAZ), heat-affected zone (HAZ) and base metal. FSW results in the temperature increase up to 400−550 °C within the nugget zone. At such a high temperature, precipitates can coarsen or dissolve into aluminum matrix which depends on the type of alloy and the maximum temperature [5]. Therefore, the need of applying heat treatment after welding 2xxx and 7xxx series aluminum alloys is essential to achieve the desired mechanical properties. In this regard, the effect of post-weld heat treatment (PWHT) on the mechanical properties of dissimilar friction stir-welded aluminum alloys was studied. ZADPOOR et al [6] investigated mechanical properties of friction stir welding alloys produced by 2024-T3 and 7075-T6 processes. It was shown that hardness was more at the advancing side and reduced towards into the retreating side of friction steered sample. CHEN et al [7] studied the effect of welding heat input and post-welded heat treatment on hardness of stir zone for friction stir-welded 2024-T3 aluminum alloy. It was found that, under high welding heat input condition, a higher welding speed is beneficial for improving the hardness of the stir zone and hardness of the stir zone decreases after post-weld heat treatment

Corresponding author: B. SAFARBALI; Tel/Fax: +98-2833348597; E-mail: b.safarbali@ma.iut.ac.ir
DOI: 10.1016/S1003-6326(18)64766-1

due to over-aging. JAMSHIDI [8] studied the effect of post-weld heat treatment on mechanical properties of dissimilar welded AA6082 and AA7075 alloys using the friction stir welding. It was shown that, after natural aging at room temperature for a period of 8760 h, the stir zone showed the highest kinetics of hardness and strength recovery. AYDIN et al [9] examined the effect of PWHT on mechanical properties of friction stir welded 2024-T4 aluminum alloy. Post-weld heat treatment process caused abnormal grain growth in the welded zone. It was also shown that T6 aging treatment (190 °C, 10 h) had the greatest impact on improvement of mechanical properties of 2024-T4 welded joint. HU et al [10] reported that both the base metal and weld zone have large plastic deformation and reduction of elongation welded joints improved by post-weld heat treatment. BAYAZID et al [11] investigated the effects of cyclic solution treatment on microstructure and mechanical properties of friction stir welded AA7075. The cyclic solution treatment was done at a repeated heating between 400 and 480 °C for 0.25 h. Grain size did not considerably change after cyclic solution treatment. It was reported that, this heat treatment improved tensile strength and elongation of friction stirred AA7075 alloy.

Despite the mentioned studies, there is limited study about effect of post-weld heat treatment on joint properties of dissimilar AA2024 and AA 7075 alloys. Therefore, in this study, the aim is to improve the mechanical properties of the friction stir welded joint.

2 Experimental

In this study, samples made from aluminum alloys AA2024-T4 and AA7075-T6 with a thickness of 4 mm were used. The chemical compositions of these two alloys are given in Table 1. Samples were longitudinally butt-welded parallel to the rolling direction using a manual vertical milling machine. A schematic diagram of joint geometry is shown in Fig. 1. AA2024-T4 was located on the advancing side, while AA7075-T6 was located on the retreating side of the weld (see Fig. 1). The tool used for the welding was heat treated by H13 tool steel. As shown in Fig. 2, tool shoulder diameter, diameter and length of the pin in the tool were 18, 6.4 and 3.8 mm, respectively. Direction of tool rotation was selected clockwise. The tool was fixed at 3° to the longitudinal axis. The tool rotation speed was 1140 r/min, and the tool advancing rate was 32 mm/s. To measure the temperature of the welded region during the process, Cromel–Alumel type thermocouple was used. For this purpose, two thermocouples were placed on both of the advancing and retreating sides at a distance of 11 mm from the welded center. In order to apply post-weld heat treatment cycles, the samples were solution annealed at 460 °C for 2 h. After solution treatment, post-weld heat treatment procedure was done at aging conditions shown in Table 2, where, aging treatments were designated as 2024-T6, 7075-T6, T_1, T_2 and T_3, respectively. Mechanical properties of the post-weld heat treated joints were determined by performing tensile and micro-hardness tests. For this purpose, samples were prepared perpendicular to the direction of welding in accordance with the standard ASTM E8 (Fig. 3) [13].

Microstructural characterization from different areas of welded joints was done using optical microscope, scanning electron microscope (SEM) and field emission scanning electron microscope (FESEM). In this regard, specimens were etched in a solution with 5 mL nitric acid, 2 mL hydrofluoric acid, 3 mL hydrochloric acid

Table 1 Chemical compositions of aluminum alloys used in this study (mass fraction, %)

Aluminum alloy	Zn	Mg	Cu	V
AA7075-T6	5.21	2.62	1.58	0.162
AA2024-T4	−	1.443	4.089	0.01

Aluminum alloy	Cr	Ti	Mn	Fe	Al
AA7075-T6	0.391	0.116	0.165	0.163	Bal.
AA2024-T4	−	0.039	0.425	0.123	Bal.

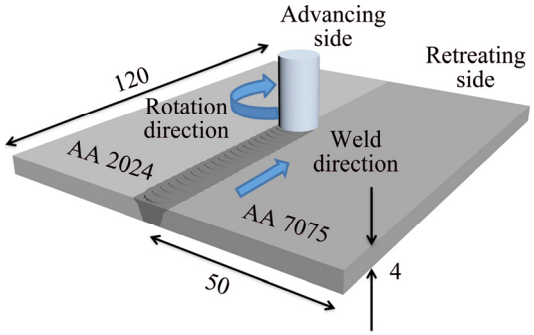

Fig. 1 Schematic diagram of joint geometry for FSW process used in this study (unit: mm)

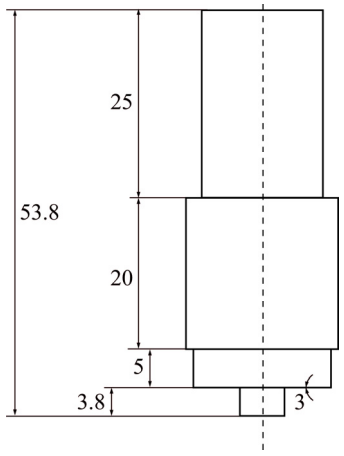

Fig. 2 Geometry of welding stir tool (unit: mm)

Table 2 Aging treatment conditions performed on as-welded joint

Treatment designation	Time/h	Temperature/°C
2024-T6	10	190
7075-T6	24	120
T_1	12	170
T_2	16	170
T_3	20	170

The aging treatment parameters were selected based on Ref. [12].

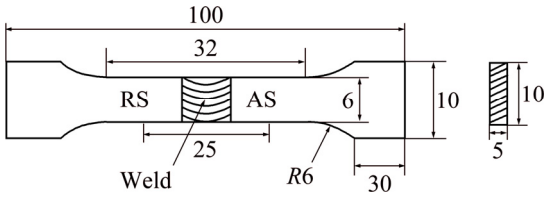

Fig. 3 Schematic diagram of tension test specimen (unit: mm)

and 190 mL distilled water. To determine possible phases formed in weld regions, a field emission scanning electron microscope (FESEM) equipped with an energy-dispersive X-ray spectroscopy (EDS) and X-ray diffraction (XRD) was used.

3 Results and discussion

3.1 Macrostructure of as-welded joints

Macroscopic appearance of cross-section of joints produced at rotation speeds of 1140 r/min and 32 mm/min is shown in Fig. 4. Friction stir welded dissimilar 2020-T4 and 7075-T6 aluminum alloys joints consist of several zones with different microstructures, i.e., SZ, TMAZ and HAZ. This is due to different thermal cycles and deformation rates in each region. Macroscopic observation showed that all joints were free from macro defects such as the tunnel defect and kissing bond defect. In fact, the welding parameters used in this study were generated enough heat flow, so that the mixing of the two alloys completely occurred. Onion ring patterns (banded structure) were slightly observed in SZ.

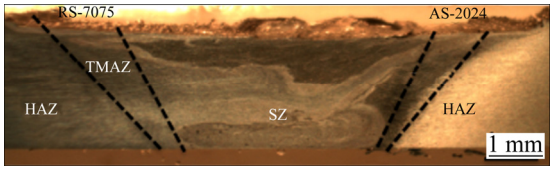

Fig. 4 Macro-structural classification of different regions in FSW zone of as-welded joints

3.2 Microstructure of as-welded joints

The microstructures of stir zone on retreating and advancing sides of weld joint are shown in Figs. 5(a) and (b), respectively. As can be already seen in Figs. 5(a) and (b), grain refinement occurs in stir zone. The simultaneous increase in heat input and severe plastic deformation has caused grain refinement in the stir zone. Also, it is clear that the grain size on the advancing side (AS) is less than that on retreating side (RS). This is due to experiencing higher temperatures of the advancing side than retreating side of stir zone during welding [5]. Moreover, band structure can be observed slightly in some areas in the stir zone. With increase of the heat input, more driving force for diffusion of alloying elements exists and the band structures are less visible [6]. However, because of the relatively high cooling rate, this structure does not completely disappear. As shown in Fig. 5(a) precipitates are dissolved in the stir zone due to the high temperatures experienced during welding in this region. Figures 5(c) and (d) show the microstructure of TMAZ on retreating and advancing sides of weld joint, respectively. As can be seen in this region, grains in the TMAZ have rotated and elongated significantly. Grain refinement has not occurred and the grain size in this area is greater than the rest in other regions. Although TMAZ is under plastic deformation, but grain refinement has not occurred in this region because of insufficient deformation strain [5]. However, as seen in Fig. 5(d) in areas close to stir zone minor recrystallization and grain refinement occur between large grains. Also precipitate coarsening occurs, as it can be clearly observed in Figs. 5(c) and (d). Figures 5(e) and (f) show microstructure of HAZ on AA2024 and AA7075 sides, respectively. In this region coarsening of precipitates occurs and grain sizes have changed slightly. However, the thermal exposure above 250 °C exerts a significant effect on the precipitate structure. This is due to that HAZ experiences a thermal cycle, but does not undergo any plastic deformation [5].

3.3 Thermal cycle in as-welded joint

Figure 6 shows the temperature cycle performed on both advancing side (AS) and retreating side (RS) of the joint. As can be seen in Fig. 6, AA2024 is located in the advancing side, which experiences higher temperature than AA7075 located in retreating side. The measured temperatures on the advancing side and retreating side were 355 and 328 °C, respectively. Similar results were reported in other studies on friction stir welding of dissimilar aluminum alloy [3]. FSW results in intense plastic deformation around rotating tool and friction between tool and work pieces. Both these factors contribute to the temperature increase within and around the stirred zone. It was also noted that there was a slightly higher temperature on the advancing side of the joint where the tangential velocity vector direction was the same as the forward velocity vector [5]. This could

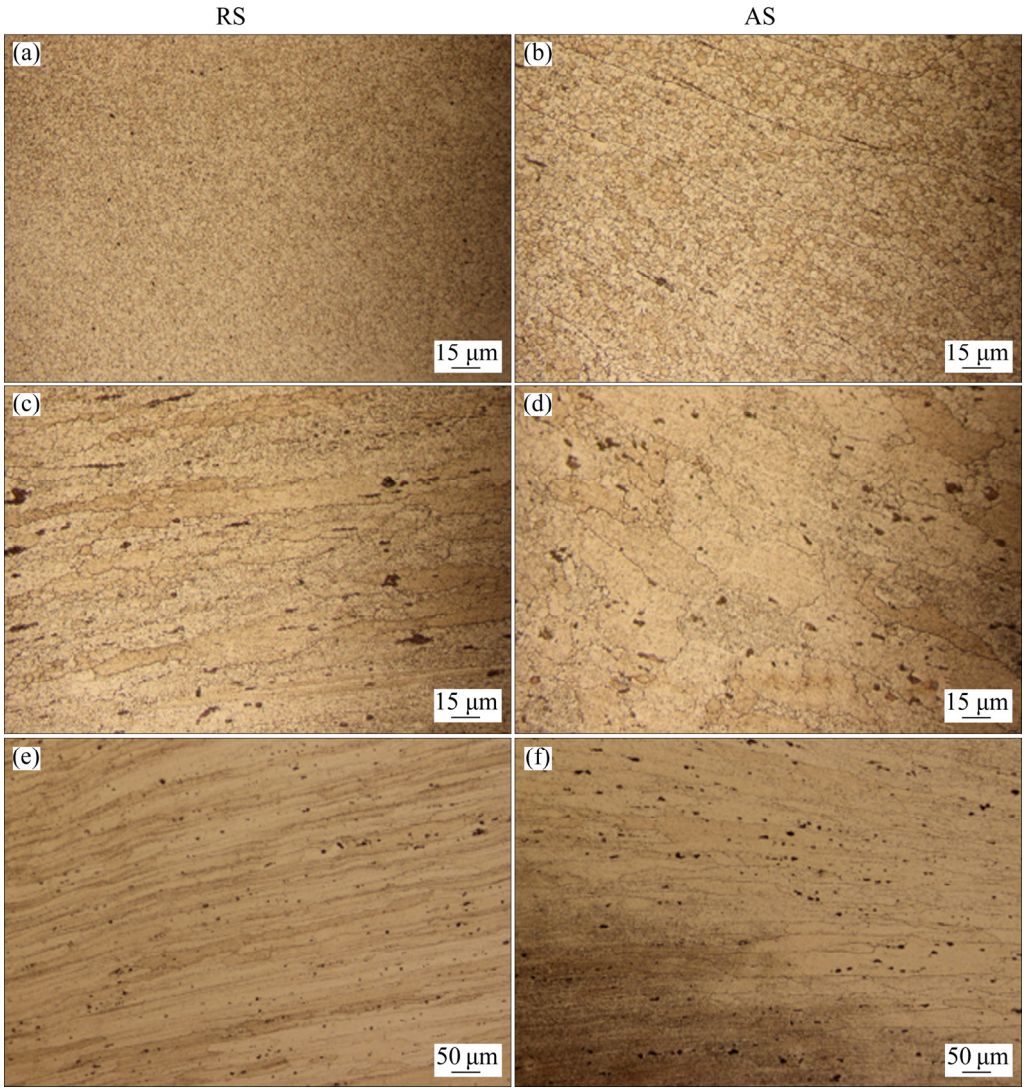

Fig. 5 Optical micrographs of FSW zone of as-welded joint: (a, b) Stir zone; (c, d) TMAZ; (e, f) HAZ

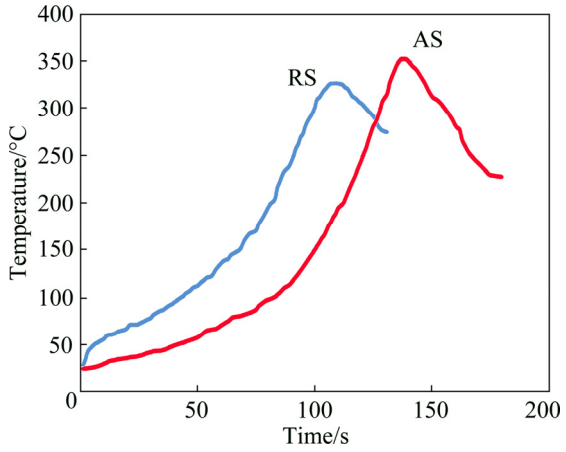

Fig. 6 Measured thermal cycles on AS and RS at distance of 11 mm from weld center

be caused that material on the advancing side experiences much more plastic deformation and higher temperature than material on the retreating side [14].

3.4 Elemental distribution and precipitates in as-welded joint

Figure 7 shows BE-SEM and FE-SEM images of precipitates in different areas of welded joint. As can be seen, precipitates are mostly dissolved in stir zone (Figs. 7(e) and (f)). On the other hand, particles in TMAZ on both sides have coarsened and distributed in the direction of grain flow on both sides of as-weld joint (Figs. 7(a)−(d)). From previous studies [9], this could be because of high temperature of 450−490 °C in the center of stir zone [9].

FE-SEM image and EDS result of particles in nugget zone are shown in Fig. 8. Particle analyses in points 1 and 4 show that these particles are strengthening precipitation and round-shape. Also, particle in point 3 has a composition close to $(Cu,Fe,Mn)Al_6$ that these compounds have stretched-shape. The amount of these elements in the stir zone is less than that in the TMAZ and HAZ. According to Refs. [15,16], there are two

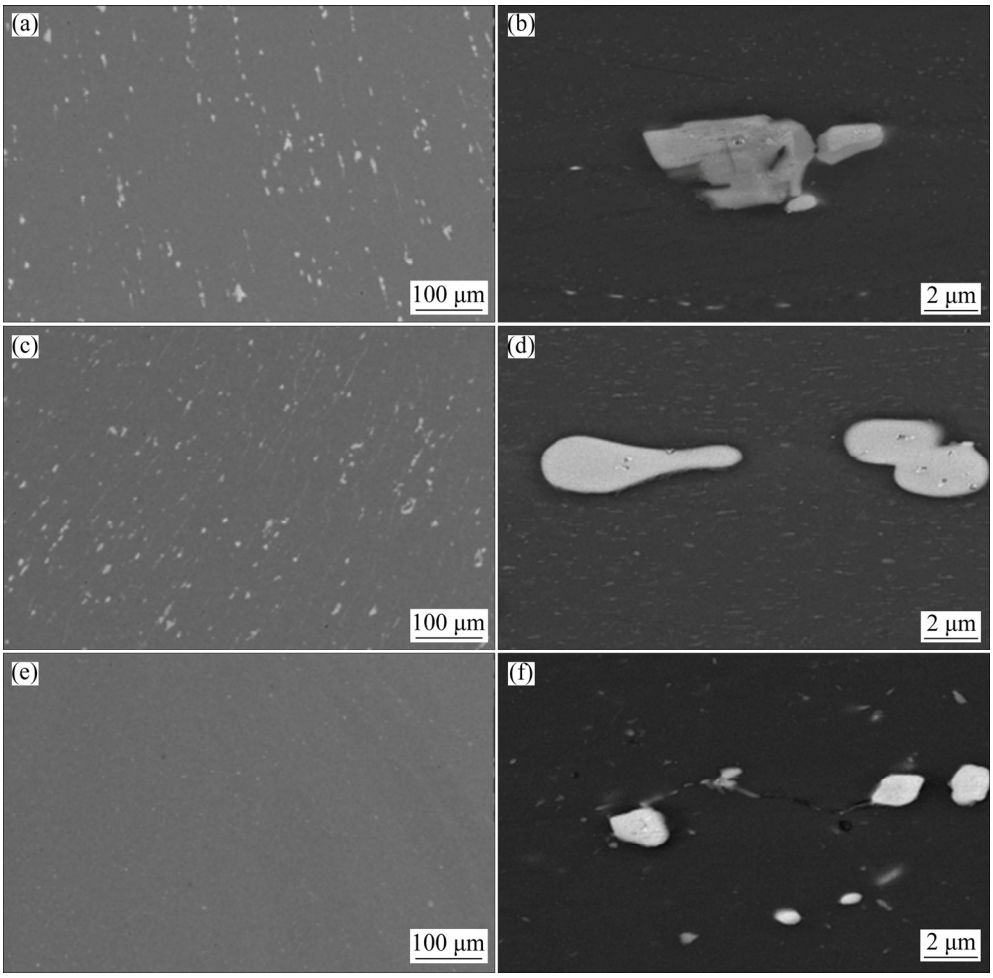

Fig. 7 BE-SEM (a, c, e) and FE-SEM (b, d, f) images of precipitates in as-welded joint: (a, b) TMAZ of advancing side; (c, d) TMAZ of retreating side; (e, f) Nugget zone

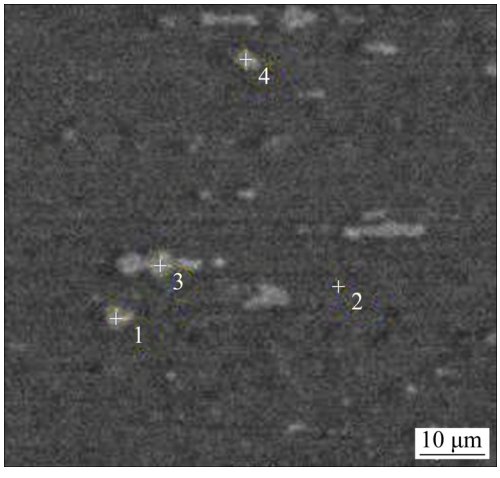

Point	x(Mg)/%	x(Al)/%	x(Cu)/%	x(Zn)/%	x(Mn)/%	x(Fe)/%	Total/%
1	19.61	52.72	25.57	2.11	−	−	100
2	3.49	93.93	2.58	−	−	−	100
3	2.80	64.44	34.04	3.16	5.17	10.18	100
4	19.62	55.66	22.95	1.78	−	−	100

Fig. 8 BE-SEM image and EDS analysis of different particles in nugget zone of as-welded joint

different types of particles in the as-weld joint of aluminum alloys. These are precipitation-hardening compounds such as $S(Al_2CuMg)$ and $\eta(MgZn_2)$ or compounds containing Fe and Mn, such as $(Cu,Fe,Mn)Al_6$ [15,16]. It is known that strengthening precipitates, such as rod or lath shaped Al_2CuMg, can coarsen or dissolve during high temperature heat treatment, while particles containing Fe and Mn are insoluble in aluminum alloys [17]. Particles shown in SEM image in Fig. 8 contain these elements.

3.5 Effect of aging treatment on microstructure

Figures 9(a)−(c) show cross-sectional images of the welded joints subjected to 2024-T6 treatment. Optical images show abnormal grain growth phenomenon formed during 2024-T6 treatment especially in TMAZ on retreating side (AA7075). As mentioned above, after solution treatment, certain changes take place in the microstructure of friction stir welded joint. Grain growth appears to be a natural consequence of heat treatment [18]. Abnormal grain growth in some areas could be attributed to the fact that the thermodynamic

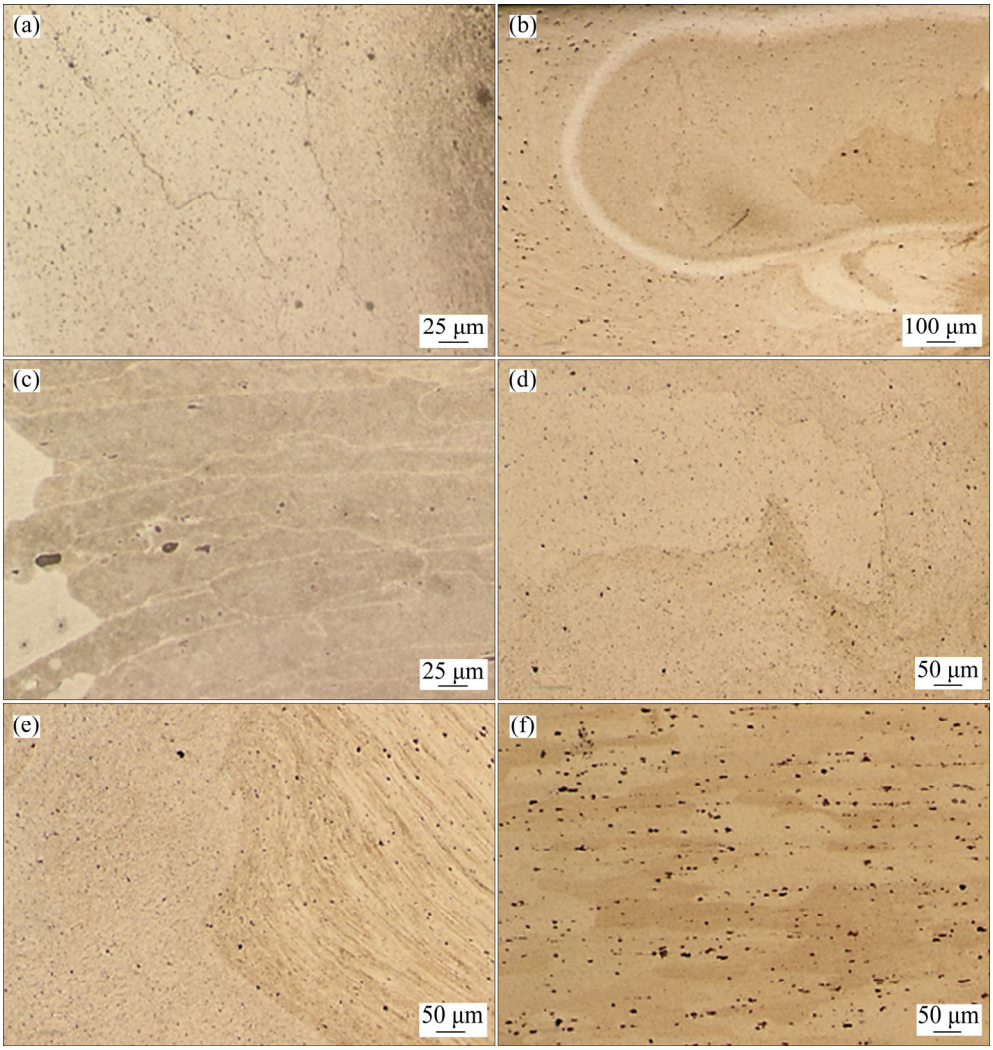

Fig. 9 Optical micrographs of weld zones subjected to different PWHTs: (a−c) 2024-T6; (d−f) 7075-T6; (a, d) Stir zone; (b, e) TMAZ of AA7075; (c, f) TMAZ of AA2024

driving force for abnormal grain growth is higher than the pinning force that impedes grain boundary migration [19]. Reduction of pinning force is a result of precipitates dissolution at high temperature during friction stir welding process. Grain structure on TMAZ on advancing side (AA2024) is shown in Fig. 9(c). In comparison with stir zone, intensity of grain growth has reduced in TMAZ due to lower temperature during welding. In addition, after heat treatment of the weld zone, rotation and stretch of grains decreased. However, size and distribution of the hardening precipitates were varied significantly in the friction stir-welded zone of the joints depending on the PWHT conditions. The morphology and distribution of precipitates in the welding zone are shown in FESEM (Fig. 10). Considering that temperature of 2024-T6 treatment is 190 °C, which is above the aging temperature of AA7075, and its maximum strength is obtained at 120 °C. In fact, 2024-T6 treatment has caused coarsening of precipitates in AA7075 (see Fig. 10(a)).

Microstructures of different regions of friction stir weld after 7075-T6 treatment are shown in Figs. 10(d)−(f). As can be seen, grains have grown in the stir zone of joint similar to 2024-T6, but the intensity is lower. 7075-T6 procedure is suitable for AA7075, since fine and uniform distribution of strengthening precipitates such as $MgZn_2$ is formed in the TMAZ of AA7075 (Fig. 10(d)). In the TMAZ of AA2024 some coarsening precipitates can be seen (Fig. 10(f)). For conventional 7075-T6, the selected temperature is 120 °C which is low for aging of AA2024, Therefore, over aging does not occur in AA2024. As a result, mechanical properties of the AA2024 are not affected by 7075-T6 treatment.

3.6 Micro-hardness of as-welded and PWHT joints

Hardness profile in the cross-section of friction stir welded joint after heat treatment is shown in Fig. 11. The

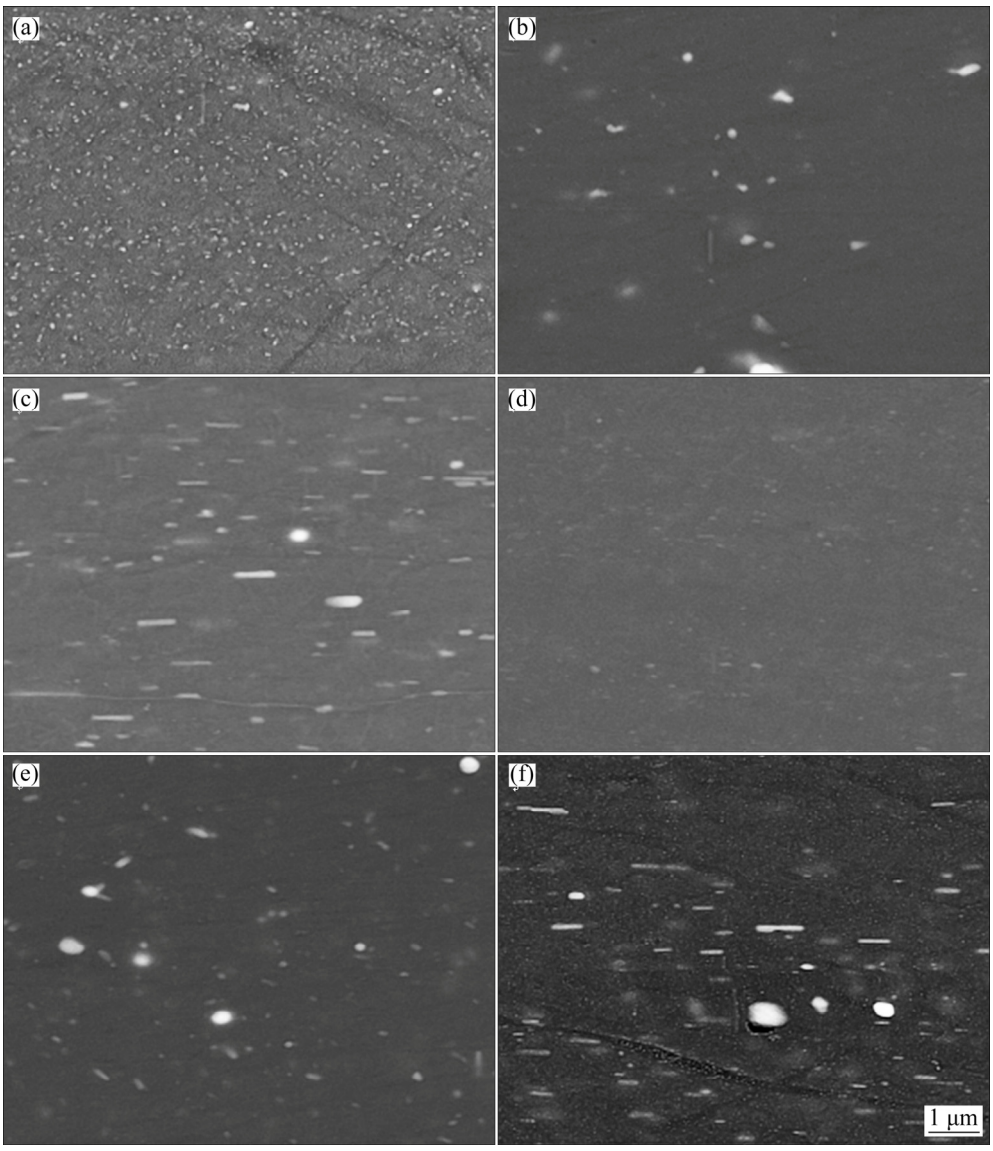

Fig. 10 FE-SEM images from welding zone of FSWed joint after PWHT showing distribution of precipitates: (a−c) 2024-T6; (d−f) 7075-T6; (a, d) TMAZ of AA7075; (b, e) Nugget zone; (c, f) TMAZ of AA2024

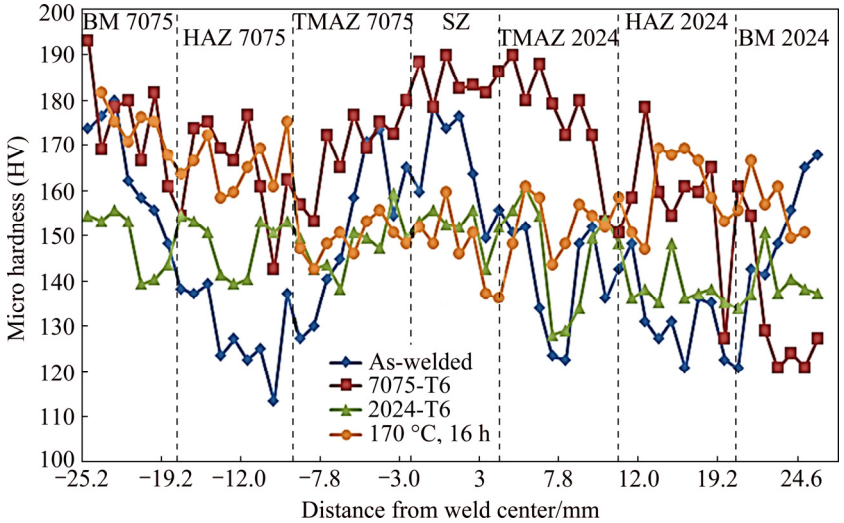

Fig. 11 Micro-hardness profiles of as-weld joint under various PWHT conditions from transverse to welding direction

micro-hardness profile of as-welded joint shows a general softening in the TMAZ and HAZ in contrast to base metal (BM) and nugget zone (NZ). The transition zone between the TMAZ and HAZ of the as-welded joint has a hardness of HV 110, while the hardness in the NZ is about HV 160 (Fig. 11). The reason of hardness loss in the TMAZ and HAZ is the coarsening and over-aging of hardening precipitates as a result of the weld thermal cycle during the FSW process. After welding, continuous dynamic recrystallization results in fine-equiaxed grains in stir zone [5]. Therefore, despite precipitate dissolution, the hardness in nugget zone of as-weld joint is higher than that in HAZ and TMAZ, and is lower than that of the base metal. It is remarkable that the drop in hardness of transition zone between HAZ and TMAZ on the retreating side (AA7075) is lower than that in the area on advancing side (AA2024), although hardness of AA7075-T6 before welding is higher than that of AA2024-T4. This could be because that hardening precipitates in AA7075 have inferior thermal stability and are solved at a lower temperature than that in AA2024.

Hardness values across the weld zone of PWHT joints vary depending on the PWHT procedures as shown in Fig. 11. The hardness across the weld zones of joints after 2024-T6 treatment is the lowest in comparison to other areas. The hardness decreases in stir zone in comparison with that of as-welded joint. Hardness slightly increases in TMAZ and HAZ on both sides and is close to HV 140 (Fig. 11). This can be due to over-aged strengthening precipitates such as $MgZn_2$ in AA7075. Among other PWHT processes, 7075-T6 treatment has the greatest increase in hardness in weld zone. This enhancement in hardness is due to the formation of fine and uniform precipitate distribution in all areas of joint. The reason of moderate hardness increasing in 170 °C and 16 h (T_2) condition is that high temperature (170 °C) caused over-aging in AA7075 and selected time period is not enough to obtain maximum hardness in AA2024. Aging at 170 °C for 16 h (T_2) causes equally improvement of hardness on both sides compared with as-welded joint. Also, in all samples, hardness recovery in the stir zones was faster than that in TMAZ. This could be due to the high concentration of vacancies and solute saturation in the stir zone [20].

3.7 Phase characterization of as-welded and PWHT joints

Figure 12 shows X-ray diffraction (XRD) patterns in nugget zone of joints under various conditions. According to Fig. 12(a), strengthening precipitates such as $MgZn_2$ and Al_2CuMg have dissolved in as-welded joint and only particles that contain elements such as Fe ($FeAl_3$ compound) remain in the structure. After PWHT, the hardening precipitates such as $MgZn_2$ and Al_2CuMg nucleate and grow. According to XRD results by applying 2024-T6 aging treatment, Al_2CuMg particles distinguish (Fig. 12(b)). Some peaks in Fig. 12(b) also show possibility of the formation of $MgZn_2$ during PWHT. Also, as can be seen in Fig. 12(c) by applying 7075-T6 treatment, $MgZn_2$ has been diagnosed after PWHT. Al_2CuMg and $MgZn_2$ precipitates are known as strengthening precipitates [14,15]. Since temperature and time of 7075-T6 treatment are not enough for the formation of *S*(Al_2CuMg) in AA2024, they are not detected in XRD patterns (Fig. 12(c)).

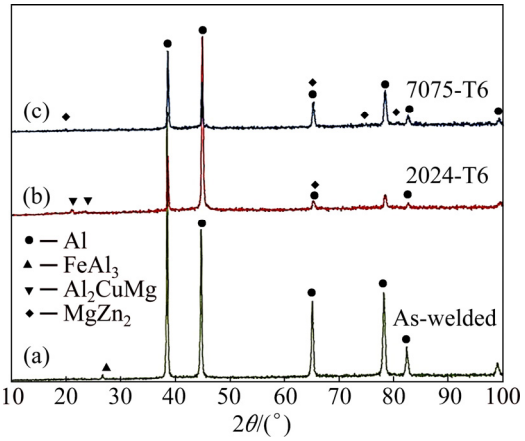

Fig. 12 XRD patterns of nugget zone of welds

3.8 Tensile properties of as-welded and PWHT joints

The tensile properties of as-welded and PWHT joints are shown in Table 3. The un-welded AA7075 and AA2024 metals have tensile strength of 570 and 426 MPa, respectively. Also, the elongation and tensile strength of the as-welded joint are 9.6% and 381 MPa, respectively. This indicates 34% and 11% reduction in strength for the dissimilar friction stir-welded joints compared with those of the AA7075 and AA2024 un-welded parent metals, respectively. The tensile tests reveal that the improvement in the tensile properties varies depending on PWHT joint conditions. The strength of PWHT welded joint based on 7075-T6 treatment has significantly increased. The yield and tensile strengths of the joint in 7075-T6 treatment are 349 and 453 MPa, respectively. The yield and ultimate tensile strengths for 2024-T6 aging treatment are 311 and 406 MPa, respectively, which shows slight increase in comparison to as-welded joint. Also, the aging treatment at 170 °C for16 h (T_2) offers the highest strength recovery than that after aging treatment for 12 and 20 h (Table 3). After 7075-T6 treatment increase in elongation was also observed (Table 3). The improved strength and elongation after 7075-T6 treatment resulted in increase in toughness of the welded joint. This is an indication of formation of fine and uniform hardening precipitates. It

is well known that strength in the presence of precipitates increases by pinning of grain boundaries and by also dislocation motion [21]. In other procedure, reduction of ductility is attributed to the abnormal grain growth and coarsening of hardening precipitate (especially $MgZn_2$). Therefore, the static properties of the friction stir-welded joints of the precipitation-hardening alloys depend on the distribution of the hardening precipitates rather than the grain size [22].

Table 3 Tensile properties of FSWed 2024 and 7075 Al alloy joints before and after aging treatment

Specimen condition	Ultimate tensile strength/MPa	Tensile yield stress/MPa	Elongation/ %
As-welded	381	302	9.6
2024-T6	406	311	7.36
7075-T6	453	349	15.2
170 °C, 12 h (T_1)	443	322	5.6
170 °C, 16 h (T_2)	448	334	6.7
170 °C, 20 h (T_3)	429	318	7.1

Failure of weld joints before heat treatment located in the transition zone between TMAZ and HAZ on the retreating side (AA7075). The 7075-T6 treatment makes significant improvement of strength in this area as the weakest part of the weld zones. In other process, the strength slightly increased since temperature and time were not suitable for aging of AA7075 (170, 190 °C). In all samples after PWHT, fracture occurred in the stir zone because of abnormal grain growth after the solution treatment.

3.9 Fracture surfaces of as-welded and PWHT joints

The fracture surfaces of the as-weld, PWHT joints based on 7075-T6 and 2024-T6 treatment after tensile test taken from central region are shown in Fig. 13. It can be seen from Fig. 13, that fractures in PWHT samples are predominantly inter-granular while in as-weld joint the fractures of joints are mostly trans-granular. This fracture behavior is associated with coarsening and dissolution of precipitates in TMAZ and HAZ during welding [11]. In addition, brittle particles containing Fe, Mn, Cr elements remained in the structure after the welding process. Therefore, the interface between the brittle compound and matrix could play an important role as initiator and propagator of cracks. This leads to the strength reduction within the grains in comparison with grain boundaries.

By applying PWHT process, precipitation nucleation and growth has initiated and uniformly distributed. Precipitates are formed within the grains after PWHT. This results in more effective strengthening of grains than grain boundaries. In this regard, after PWHT inter-granular fracture occurred more than trans-granular fracture. Also, the type of PWHT procedure affected the amount of ductility. It is reported that size and depth of the dimples on the fracture surfaces are related with ductility [23]. The size of the dimples on the fracture surface of as-weld joint is larger than PWHT joints (see Fig. 13(a)). This suggests that a large stretch zone is present at the tip of the crack. This led to a large plastic zone ahead of the crack and high ductility [24]. By comparing the fracture surfaces of PWHT joints, it is identified that dimples in 7075-T6 treatment are deeper than those in 2024-T6 (see Fig. 13(b)). As mentioned above, this is due to the formation of fine and uniformed precipitates after the 7075-T6 treatment.

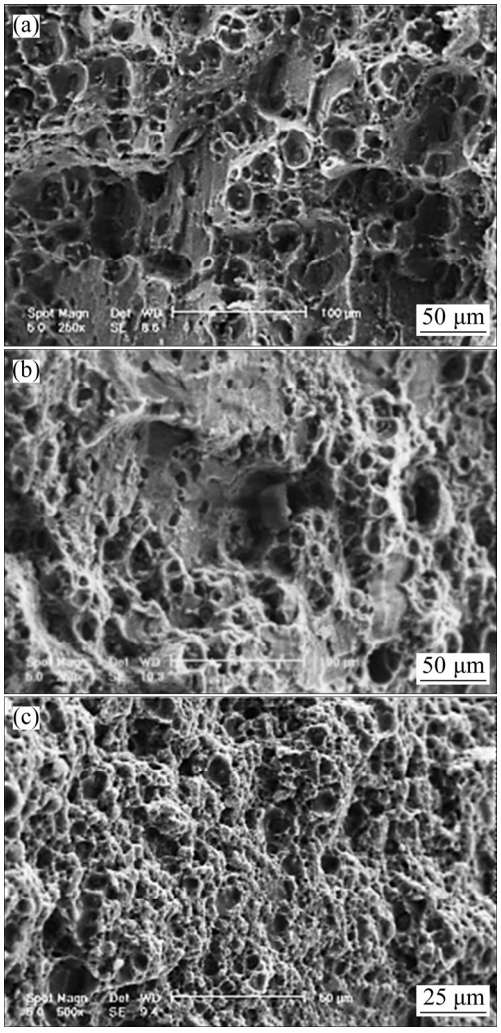

Fig. 13 SE-SEM images showing fracture surface of joints after tensile testing: (a) As-welded; (b) 7075-T6; (c) 2024-T6

4 Conclusions

The effects of heat treatment after friction stir welding dissimilar welds 7075-T6 and 2024-T4 aluminum alloys were investigated. Microstructure

observation showed that precipitations were mostly dissolved in the stir zone and only particles including Fe and Mn remained in the stir zone after welding. In TMAZ on the retreating side (AA7075), more coarsening precipitations were observed. It was found that PWHT welded joint based on T6-7075 treatment had the greatest effect on enhancement tensile properties and recovery hardness. This was attributed to the formation of fine and uniform hardening precipitates ($MgZn_2$). Fracture of as-weld joints occurred in the transition zone between TMAZ and HAZ on the retreating side (AA7075), while with performing PWHT, fracture occurred in the stir zone of welded joints. This was attributed to the abnormal grain growth after solution treatment in this region. Also, fracture surface of PWHT samples was predominantly inter-granular, while for as-welded joint the fracture of joints mostly was trans-granular. This was explained by dissolution or coarsening of precipitates within grains in FSW regions during welding.

Acknowledgements

The authors would like to thank Isfahan University of Technology for its financial support.

References

[1] MATHERS G. The welding of aluminum and its alloys [M]. 1st ed. Cambridge, England: Woodhead Publishing, 2002.

[2] ZAMAN KHAN N, SIDDIQUEE A, ZAHID A. Investigations on tunneling and kissing bond defects in FSW joints for dissimilar aluminum alloys [J]. Journal of Alloys and Compounds, 2015; 648: 360−367.

[3] AMANCIO-FILHO S T, SHEIKHI S, DOS SANTOS J F. Preliminary study on the microstructure and mechanical properties of dissimilar friction stir welds in aircraft aluminum alloys 2024-T351 and 6056-T4 [J]. Journal of Materials Processing Technology, 2008; 206: 132−142.

[4] SONG Y, YNNG X, CUI L. Defect features and mechanical properties of friction stir lap welded dissimilar AA2024−AA7075 aluminum alloy sheets [J]. Materials and Design, 2014, 55: 9−18.

[5] MISHRA R S Jr. Friction stir welding and processing [J]. Materials Science and Engineering R, 2005, 50(1−2): 1−78.

[6] ZADPOOR A, SNIKE J, BENEDICTUS R. Mechanical properties and microstructure of friction stir welded tailor-made blanks [J]. Materials Science & Engineering A, 2008, 494: 281−290.

[7] CHEN Yu, DING Hua, LI Ji-zhong, ZHAO Jing-wei, FU Ming-jie, LI Xiao-hua. Effect of welding heat input and post-welded heat treatment on hardness of stir zone for friction stir-welded 2024-T3 aluminum alloy [J]. Transactions of Nonferrous Metals Society of China, 2015, 25: 2524−2532.

[8] JAMSHIDI A H. Influences of pin profile on the mechanical and microstructural behaviors in dissimilar friction stir welded AA6082–AA7075 butt joint [J]. Materials and Design, 2015; 67: 413−421.

[9] AYDIN H, BAYRAM A, DURGUN I. The effect of post-weld heat treatment on the mechanical properties of 2024-T4 friction stir-welded joints [J]. Materials and Design, 2010, 31: 2568−2577.

[10] HU Zhi-li, YUAN Shi-jian, WANG Xiao-song, LIU Gang, HUANG Yong-xian. Effect of post-weld heat treatment on the microstructure and plastic deformation behavior of friction stir welded 2024 [J]. Materials and Design, 2011; 32: 5050−5050.

[11] BAYAZID S M, FARHANGI H, ASGHARZADEH H. Effect of cyclic solution treatment on microstructure and mechanical properties of friction stir welded 7075 Al alloy [J]. Materials Science & Engineering A, 2016, 649: 293−300.

[12] CHANDLER H. Heat treater's guide: Practices and procedures for nonferrous alloys [M]. Materials Park, OH, USA: ASM International, 1996.

[13] ASTM E8-04. Standard Test Methods for Tension Testing of Metallic Materials [S]. ASM International, 2007.

[14] CHO J H, BOYCE D E, DAWSON P R. Modeling strain hardening and texture evolution in friction stir welding of stainless steel [J]. Materials Science & Engineering A, 2005; 398:146−63.

[15] MONDOLFO L F. Aluminum alloys: Structure and properties [M]. London: Butterworth, 1976.

[16] BROOKS C R. Heat treatment, structure and properties of nonferrous alloys [M]. Metals Park, OH, USA: ASM International, 1984.

[17] GENEVOIS C, DESCHAMPS A, DENQUIN A, DOISNEAU-COTTIGNIES B. Quantitative investigation of precipitation and mechanical behaviour for AA2024 friction stir welds [J]. Acta Materialia, 2005, 53: 2447−58.

[18] CHARIT I, MISHRA R S. Abnormal grain growth in friction stir processed alloys [J]. Scripta Materialia, 2008, 58: 367−71.

[19] CHARIT I, MISHRA R S, MAHONEY M W. Multi-sheet structures in 7475 aluminum by friction stir welding in concert with post-weld superplastic forming [J]. Scripta Materialia, 2002, 47: 631−6.

[20] FULLER C B, MAHONEYA M W, CALABRESEA M, MICONA L. Evolution of microstructure and mechanical properties in naturally aged 7050 and 7075 Al friction stir welds [J]. Materials Science & Engineering A, 2010, 527: 2233−40.

[21] STARINK M J, DESCHAMPS A, WANG S C. The strength of friction stir welded and friction stir processed aluminum alloys [J]. Scripta Materialia, 2008, 58: 377−82.

[22] ATTALLAH M M, SALEM H G. Friction Stir welding parameters: A tool for controlling abnormal grain growth during subsequent heat treatment [J]. Materials Science & Engineering A, 2005, 391: 51−9.

[23] SRIVATSAN T S, VASUDEVAN S, PARK L. The tensile deformation and fracture behavior of friction stir welded aluminum alloy 2024 [J]. Materials Science & Engineering A, 2007, 466: 235−45.

[24] AYDIN H, BAYRAM A, UGUZ A, AKAY S K. Tensile properties of friction stir welded joints of 2024 aluminum alloys in different heat-treated-state [J]. Materials and Design, 2009, 30: 2211−21.

焊后热处理对异种金属搅拌摩擦焊 2024-T4 和 7075-T6 铝合金接头性能的影响

B. SAFARBALI, M. SHAMANIAN, A. ESLAMI

Department of Materials Engineering, Isfahan University of Technology, Isfahan 84156-83111, Iran

摘　要：研究焊后热处理对异种金属搅拌摩擦焊 AA7075 和 AA2024 接头性能的影响。在一定的参数下焊接后，对焊接接头进行固溶处理和不同的时效处理。采用光学显微镜、SEM、FE-SEM、XRD 和 EDS 表征材料的显微组织和相成分，最后测试对比热处理前后样品的力学性能。结果显示，与焊接后未热处理的接头相比，焊后热处理过程可以明显提高 2024-T6 和 7075-T6 焊接接头的力学性能，7075-T6 的力学性能提高更明显，这是因为在时效过程中形成细小沉淀相，尽管有异常晶粒长大。未热处理的 AA7075 的接头断裂发生在后退侧热机械影响区(TMAZ)和高热影响区(HAZ)的界面，而热处理后断裂位置转移到接头的搅拌区(SZ)。未热处理的接头断裂为穿晶断裂，而热处理后样品的断裂主要以晶内断裂为主，这主要是因为接头热处理后晶体内的沉淀相发生分解和粗化。

关键词：搅拌摩擦焊；异种金属焊接；焊后热处理；显微组织；力学性能

(Edited by Xiang-yun LI)